Journal of Magnetism and Magnetic Materials 488 (2019) 165364

Contents lists available at ScienceDirect

Journal of Magnetism and Magnetic Materials

journal homepage: www.elsevier.com/locate/jmmm

Research articles

Steady microwave absorption behavior of two-dimensional metal carbide MXene and Polyaniline composite in X-band

Sumit Kumar[a,b], Arti[a,b], Parveen Kumar[a,b], Nidhi Singh[c], Vivek Verma[a,*]

[a] Department of Physics, Hindu College, University of Delhi, Delhi 110007, India
[b] Department of Physics and Astrophysics, University of Delhi, Delhi 110007, India
[c] National Physical Laboratory (CSIR), Dr. K.S. Krishnan Road, New Delhi 110012, India

ARTICLE INFO

Keywords:
Electromagnetic Interference
Hydrophilic
Magnetic
MXene

ABSTRACT

Two-dimensional metal carbides and nitrides, known as MXenes, have good metallic conductivity and hydrophilic surfaces. An elegant exfoliations approach was used to prepare a two dimensional (2D) metal carbide Ti_3C_2 MXene from layered Ti_3AlC_2 MAX phase by removing 'Al' layer by chemical etching. Here, we demonstrate the potential of MXene Ti_3C_2 and its composite with Polyaniline (PANI) for EMI shielding. The morphology, phase composition, magnetic properties and microwave absorbing properties of the samples were characterized by scanning electron microscopy, X-ray diffraction, vibrating sample magnetometer and vector network analyzer respectively. Microstructure investigation using the scanning electron microscope showed an average grain size of 6 um for Ti_3C_2 MXene. The saturation magnetization of MAX and MXene phases is 49.16 emu/gm and 49.28 emu/gm respectively. The coercivity is much higher in MXene as compared to MAX phase. The Electromagnetic Shielding properties like complex permittivity, complex permeability, S-parameters and various shielding effectiveness for the MXene-PANI composite (50% wt) were studied in the microwave frequency range (8.2–12.2 GHz). A good enhanced EMI-shielding effectiveness of ≈23 dB with the sample thickness of 1.5 mm is achieved for the lightweight MXene-PANI composite.

1. Introduction

Electronic devices are getting smarter, being miniaturized and growing in number every day. Electromagnetic wave (EM) pollution, which mainly arises from the rapid development of electronic devices, has been a threat to public health and precision instruments. Any electronic device that transmits, distributes, or uses electrical energy creates electromagnetic interference (EMI) that has negative impacts on device performance and the surrounding environment. An effective EMI shielding material must both reduce undesirable emissions and protect the component from external signals. The new shielding materials meet the requirements for the next generation effective shielding mainly, light weight, minimal thickness, powerful absorption, and wide frequency bandwidth [1,2] to fulfill the rising demands in environmental protection devices, anti-electromagnetic interference (EMI) coatings [3–6]. Mainly, two mechanisms for EMI shielding can be defined, electromagnetic reflection and absorption where reflection is due to mobile charge carriers in the material such as electrons while absorption is due to electric and/or magnetic dipoles. Also we can account for the multi-reflection during the interaction of electromagnetic waves [7,8]. Both the reflection and absorption performance of the EMI shielding materials are dependent on the high electrical conductivity. When EM radiation interacts with electrical or magnetic dipoles of shielding material, it will be absorbed and turn into heat energy. For good electromagnetic interference EMI shields, the absorber plays an important role in the electromagnetic performances. Traditional absorbers, like metals and ferrites could make a strong absorption. However, the complicated morphological tailoring is needed. Besides, the thicknesses are often too thick for practical applications [9]. Carbon materials have also been used in EMI shielding applications with the advantages of low density, excellent chemical resistance and diverse microstructures [10,11]. To achieve the objective, extensive work has been done by many researchers to study polymer matrix composites with embedded conductive fillers for EMI shielding, including a silver nanowire-polyimide hybrid [12,13], graphene-polymer nanocomposites [14], and polypropylene–stainless-steel fiber composites [15]. For most of the polymer-conductive filler hybrids, the low thermal conductivity, poor heat resistance, ease of aging, and relatively high thickness usually restrict their applications in the smart and small-scale electronics fields. Therefore, it is highly desirable to develop polymer

* Corresponding author.
E-mail address: vivekverma@hinducollege.ac.in (V. Verma).

https://doi.org/10.1016/j.jmmm.2019.165364
Received 20 March 2019; Received in revised form 24 April 2019; Accepted 24 May 2019
Available online 25 May 2019
0304-8853/

matrix composites with uniform dispersions of conductive fillers having strong interfacial interactions with the polymer to achieve a good shielding effectiveness [16]. Recently, Gogotsi and co-workers prepared metallically conductive and hydrophilic 2D transition-metal carbide (MXene) film, which exhibited a good EMI-shielding performance compared to other synthetic materials with similar thicknesses [17]. MXenes are a unique family of two-dimensional (2D) transition metal carbides and/or nitrides with the formula $M_{n+1}X_nT_x$, where M is an early transition metal (e.g., Ti, Zr, V, Nb, Ta, or Mo) and X is carbon and/or nitrogen. MXene flakes are terminated with surface moieties (T_x), such as a mixture of −OH, ═O, and −F [18]. About 20 different MXenes have already been reported. Metallic conductivity and good mechanical properties coupled with hydrophilicity make them a good candidate for use in polymer composites. Till now, MXene $Ti_3C_2T_x$, has been most commonly studied and widely used in various applications with different polymer matrices. Ti_3C_2 MXene material is considered as the ideal EM shielding materials because of its ultrahigh electrical conductivity (> 4600 S/cm), high specific surface area, hydrophilicity, and flexibility [19,20]. The MXene-polymer composites exhibited improved tensile strength [21,22]. Compared with traditional functional fillers, a novel family of electrically conductive, lightweight laminated metal carbides, carbonitrides, and nitrides (collectively referred to as MXene) opens a door for the development of multifunctional applications, especially since the discovery of Ti_3C_2 MXene. The laminated Ti_3C_2 MXene with a superior specific surface area plays a dominate role in the enhanced microwave absorbing performance. Herein, we report the synthesis and EMI shielding properties of the lightweight $Ti_3C_2T_X$/PANI composites. Since Ti_3C_2 possesses higher electronic conductivity, better chemical and environmental stability, excellent mechanical properties and exhibits stable EMI shielding efficiency so it can be a suitable option in electronic devices, weapons, and robots as a shielding material. This work confirms the great potential of the few-layered MXene as great candidates in EM absorption field.

2. Experimental

There are many different protocols for synthesizing MXene materials reported in literature [23]. Synthesis of MXene ($M_{n+1}X_n$) begins with etching the A-element atomic layers (Al, Ge, Ga etc.) in a MAX phase ($M_{n+1}AX_n$ like Ti_3AlC_2, Ti_3GeC_2, Cr_2GaN etc.) from the $M_{n+1}X_n$ layers adjacent to the A-element layers. After the etching done (complete removal of the A-element layers), the solution is centrifuged and/or filtered to separate the solid MXene powder from residual contents with the help of deionized water till the pH of suspension reaches a safe value of 6–7. A pictorial representation of synthesis process of MXene (Ti_3C_2) by MAX (Ti_3AlC_2) is given in Fig. 1. Exfoliation of the powder is also a necessary step for synthesis of MXene which can be done by ultrasonication in an organic solvent (methanol, propylene carbonate etc.).

2.1. Synthesis of MXene Ti_3C_2

High purity MAX phase Ti_3AlC_2 (make) was used to synthesis MXene Ti_3C_2. Obtained MAX was annealed in Argon atmosphere at 1300 °C for 5 h as Ti_3AlC_2 is stable at 1350 °C or even higher temperatures. One gram of the sintered powder was added to 10 ml 48% HF, stirring for 2 h at room temperature [24,25]. After etching, the suspension was filtered, dispersed in water, and filtrated again. It is extremely important to take safety protocols and to be aware of risks while handling with hazardous HF. The washing procedure was repeated 5–6 times by using centrifuge rotator with 2500 rpm to remove any remaining acid and/or reaction byproducts. The obtained powder was sonicated in the presence of methanol and dried at room temperature. The obtained Ti_3C_2 powder was kept for further experiments and characterization.

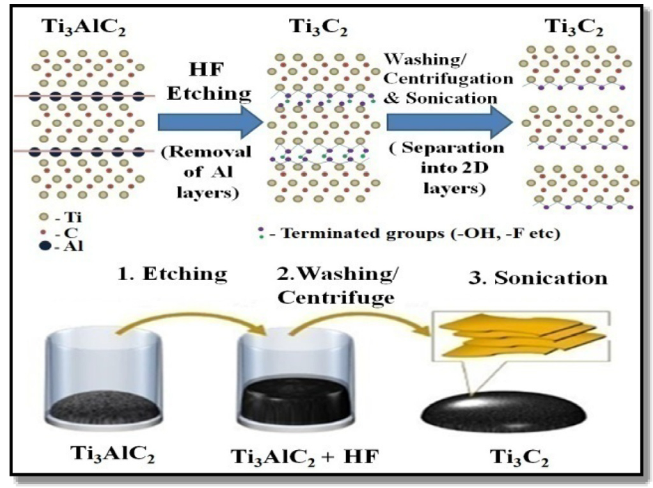

Fig. 1. Schematic route for synthesis of MXenes from MAX phases by etching and sonication.

2.2. Synthesis of PANI

Polyaniline (PANI) in emeraldine state was prepared by the chemical oxidation of aniline monomer in aqueous solution of hydrochloric acid. In a typical procedure, aniline (0.2 M) dissolved in 100 ml of HCl (1 M) was taken in 250 ml round bottom flask and stirred well. The reaction occurred in ice bath and the pre-cooled solution of ammonium persulfate (0.25 M) was slowly added over a period of 2 h as an oxidizing agent. The reaction was allowed to proceed for 6–8 h, below 5 °C [26,27]. At the end of the reaction, a dark green suspension of Polyaniline was formed. Obtained suspension was filtered and washed with deionized water and propanol several times to get pure conducting polyaniline powder.

2.3. Synthesis of composite

The composite was prepared by mechanical blending of polyaniline powder with MXene powder in 1:1 wt ratio. Due to the equal concentration of both materials, there should be better interfacial interaction between them [28]. The rectangular sample of parameter 25 × 12 × 1.5 mm was prepared using hydraulic press to calculate shielding parameters in X-band.

2.4. Characterization

XRD patterns for structural analysis of MAX (as purchased), MAX (sintered in argon atmosphere) and MXene were carried out using a Bruker D4 X-ray diffractometer with Cu-Kα radiation having wavelength $\lambda = 1.5406$ Å in the range $2\theta = 5 - 80°$.The surface morphology of all the samples was investigated by SEM (JEOL SEM 450, 30 kV). The magnetic properties of the samples were recorded by vibrating sample magnetometer (Lakeshore, 7410). The EMI shielding properties were measured by a vector network analyzer (Agilent PNAN5244A) using the waveguide method in frequency range of 8.2–12.2 GHz.

3. Results and discussions

3.1. X-ray Diffraction:

X-ray diffraction patterns for the Ti_3AlC_2 powder (MAX as obtained), Ti_3AlC_2 (MAX sintered in Ar atmosphere), Ti_3C_2 (MXene prepared from the sintered MAX powder) and Polyaniline are illustrated in Fig. 2. MAX powder (as obtained) showed a maximum intensity peak at around $2\theta = 40°$ and two other low intense peaks as shown in Fig. 2(a)

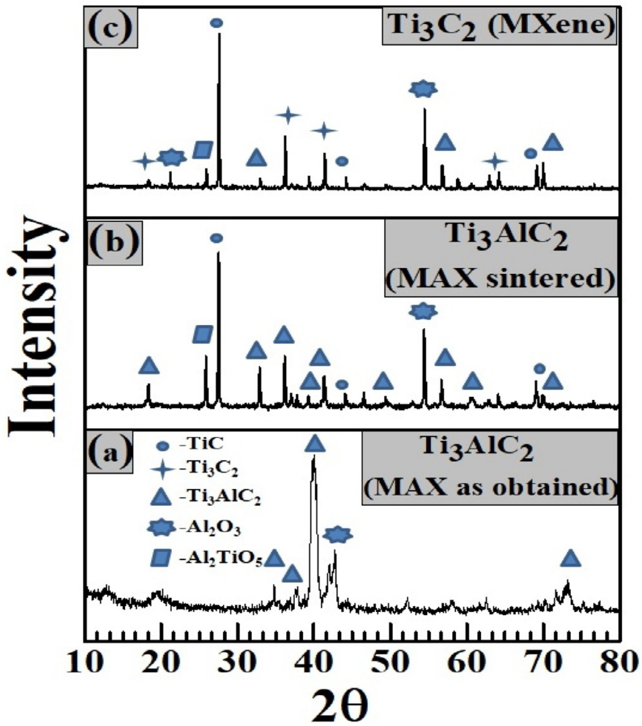

Fig. 2. XRD Patterns of (a) as obtained Ti_3AlC_2 (b) Annealed Ti_3AlC_2 (c) Ti_3C_2 in the 2θ range 5–80°.

which indicated the presence of Ti_3AlC_2 phase with the existence of Al_2O_3 impurity. To obtain the pure MAX phase, the sample was sintered in argon atmosphere at 1300 °C for 5 h. XRD patterns of Ti_3AlC_2 and Ti_3C_2 depicted an existence of mixed phase with the impurities like Ti_2AlC, TiC, $TiAl_2O_5$ and Al_2O_3 which can be considered due to the fact that titanium is a very reactive element [29,30]. Considerable loss in crystallinity and structural order is observed in the XRD pattern of the MAX sample after HF treatment. A common impurity in Ti_3AlC_2 is Ti_2AlC. The coexistence of Ti_2AlC MAX phase in Ti_3AlC_2 can lead to a mixed phase MXene of Ti_3C_2 with Ti_2C which is depicted in Fig. 2(c). The presence of Al impurities in XRD patterns of Ti_3AlC_2 and Ti_3C_2 maybe because the residual Al^{3+} will follow the migration of inside water to the surface and separate out during the oven-drying process, forming an Al_2O_3 or $TiAl_2O_5$ nanocrystals. Ti_3AlC_2 phase vanished after chemical etched using a HF solution for 2 h and replaced by Ti_3C_2 phase given by the reaction, $Ti_3AlC_2 + 3HF \rightarrow AlF_3 + 3/2H_2 + Ti_3C_2$.

The formation of extra phases with Ti_3C_2 can be reduced by ultrasonication in methanol which leads to exfoliation of MXene Ti_3C_2. XRD patterns of the conducting polymer polyaniline and the composite of Ti_3C_2 with the polymer are shown in Fig. 3. XRD pattern of Polyaniline (Fig. 3a) indicates the amorphous state with diffraction peak centered at around 2θ = 25.1°. The curve indicates that the polymeric chains are strongly disordered. The observed peak at 2θ = 25.1° is due to the presence of benzenoid and quinoid rings of Polyaniline chain. Fig. 3(b) shows the obtained XRD pattern of the composite sample with a intensity change as compared to the pure Ti_3C_2 graph and indicates a peak for the polymer addition around 25°.

3.2. Surface properties

The microstructure characteristics of the samples are revealed by SEM micrographs as shown in Fig. 4. SEM image shown in Fig. 4(a) reveals the microstructure of Ti_3AlC_2 (as obtained) which consists of uniform grains with an average grain size of 6 µm. Fig. 4(b) shows the typical morphology of layered Ti_3AlC_2 (MAX annealed at 1300 °C) with agglomeration of various impurities [31]. The SEM image of layered

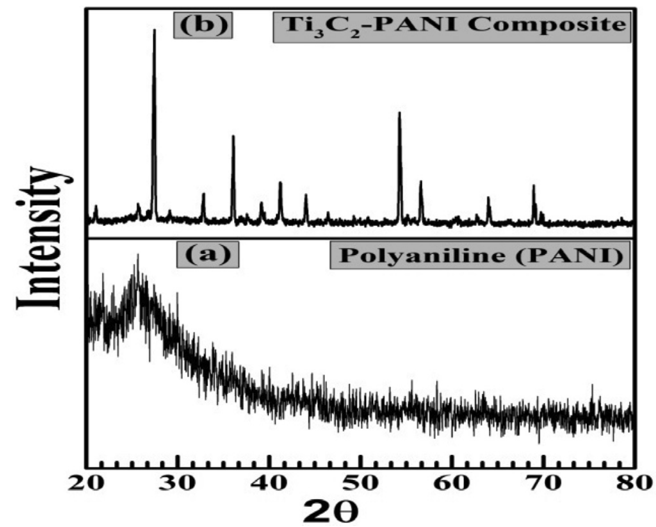

Fig. 3. XRD pattern of (a) Polyaniline in the 2θ range 20–80° (b) Ti_3C_2-PANI composite.

Ti_3C_2 (Fig. 4c), confirms the successful exfoliation of Ti_3C_2 similar with reported exfoliation [32], where Al layers have been selectively etched and the whole grains are exfoliated into massive stacked layers. Some blisters are observed on the surface of the exfoliated MXene, which may be due to the bubbles liberated due to the release of H_2 gas during the etching of the MAX phase in the presence of HF [33].

The chemical composition of Ti_3C_2 (MXene) surface is determined by X-ray photoelectron spectroscopy (XPS) depicted in Fig. 5. It can be observed from the Fig. 5(a) that the sample has the presence of Ti, C and O elements. Figure shows the peaks located at 284.4 eV which corresponds to C 1s state, at around 460 eV corresponding to Ti 2p states and at 530 eV attributed to O 1s state. In addition the peaks located at 50.1 eV and 55.4 eV corresponds to Ti 3p and 3s state respectively. Ti 2p core level shown in Fig. 5(b) exhibits two predominant peaks at 458.2 and 464.3 eV, which correspond to Ti $2p_{3/2}$ (Ti-O bonds) and Ti $2p_{1/2}$ (Ti-C bonds) respectively. The presence of Ti–C and Ti–O bonds depict the formation of Ti_3C_2 MXene. The O 1s peak suggests the presence of attached OH functional group to Ti_3C_2 as mentioned earlier, which cause polarization relaxations useful for microwave absorption performance.

3.3. Magnetic properties

The magnetic properties of the samples Ti_3AlC_2 (as obtained), Ti_3AlC_2 sintered in Ar atmosphere and the MXene (Ti_3C_2) were investigated by VSM at room temperature. Fig. 6 shows the magnetization (M) versus the applied magnetic field (± 2T) curves for all the samples. The M-H loops of the samples exhibits clear hysteresis behavior. The magnetic parameters such as saturation magnetization (Ms), remnant magnetization (Mr) and coercivity (Hc) have been determined by the hysteresis loops are given in Table 1. Ti_3AlC_2 (as obtained) shows a soft magnetic behavior with saturation magnetization value of ~2.4 emu/gm. From the Table 1 it is clear that saturation magnetization of Ti_3AlC_2 (sintered) and Ti_3C_2 are almost same with values 49.16 emu/gm and 49.28 emu/gm respectively. Ti_3C_2 shows high coercivity having value 2740 Oe in comparison to Ti_3AlC_2 having coercivity 287 Oe. This might be due to the etching in presence of HF which removes the Al layer from the MAX precursor which increases the orderness in the sample and also the reduction in the particle size with the removal of al layers. Ti_3C_2 has the layered structure with the presence electrically conductive groups on the surface of layers which may contribute to the increase in its coercivity. As per our best knowledge, till now magnetic properties have not been reported for these MAX or MXene phase samples.

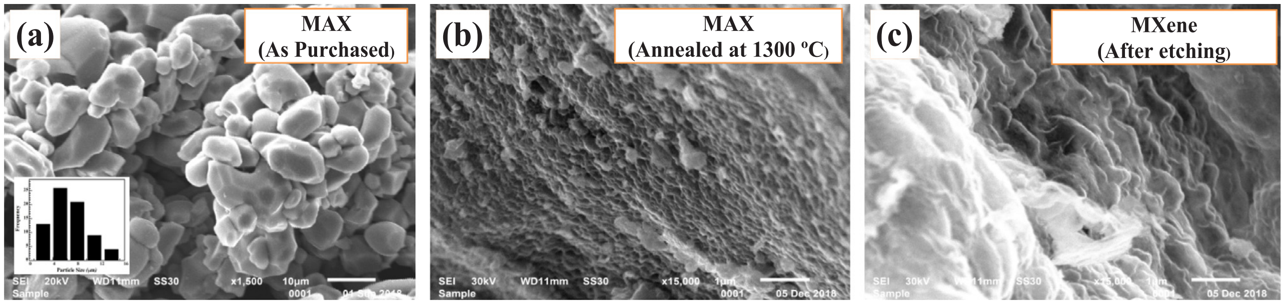

Fig. 4. SEM images of MAX and MXene powders studied here. SEM of (a) Ti_3AlC_2 (MAX as obtained) (b) Ti_3AlC_2 (MAX Annealed) (c) Ti_3C_2.

3.4. Shielding properties

To understand the probable microwave absorption property, the relative complex permittivity ($\varepsilon_r = \varepsilon' - j\varepsilon''$), relative complex permeability ($\mu_r = \mu' - j\mu''$) and shielding effectiveness (mainly consisting of reflection and absorption) of the MXene-PANI composite have been measured from VNA in the X-band (8.2–12.2 GHz) frequency range. Fig. 7 shows the real and complex parts of electrical permittivity and magnetic permeability and their tangent losses.

The relative complex permittivity with the real part denoted as ε' which represents the storage ability of electromagnetic energy, imaginary part denoted as ε“ which gives the energy dissipation and tangent loss denoted as tan $\delta = \varepsilon''/\varepsilon'$ have been investigated for Ti_3C_2-PANI composite. As illustrated in Fig. 7a and b, it is obvious that the ε' and ε“ values are high due to high conductivity of Ti_3C_2 and also due to the composite formation with a conducting polymer. Also the variation in permittivity at 10.4 GHz can be attributed to the typical dielectric relaxation behavior which may be due to the micro dipole relaxation and/or hopping migration relaxation [34,35]. Also the magnetic losses (Fig. 7d and e) have an important role in microwave absorption, which can be theoretically explained from domain wall resonance, hysteresis loss, natural resonance and eddy current effect [36,37]. The tanδ curves (Fig. 7c and f), which are used to measure the EM dissipation capability of samples, also show large values which can be explained on the highly conductive nature of composite sample which leads to presence of active polar groups in the polymer matrix. Presence of charge carriers in the defective places and the presence of functional groups form many dipoles under the presence of alternating EM field. The electrical tanδ plot (Fig. 7c) of composite slightly fluctuates over 10–11 GHz which mainly arises from the polarization. From Fig. 7f, the magnetic tangent loss of composite show the similar trend to the imaginary part of permeability. It is widely considered that loss tangent tanδ (i.e. ratio of imaginary to real part) is one of the typical physical quantities to characterize the microwave absorbing performance as higher the loss tangent which leads to enhanced seriousness of the impedance mismatch between air and the absorber.

The power coefficients of reflection (R), transmission (T), and absorption (A) for the electromagnetic shielding can be calculated using the scattering parameters, usually called as S-parameters (S_{11}, S_{12}, S_{21} and S_{22}) observed from VNA. The variation of these parameters along a shielding material placed in an EM energy source can be represented by Fig. 8. The total electromagnetic interference shielding effectiveness (EMI SE_T) is calculated by using the following equations [38,39],

$$SE_T = SE_A + SE_R + SE_M$$

$$SE_R = -10\log(1-R) = -10\log(1 - |S_{11}|^2)$$

$$SE_A = -10\log(1 - A_{eff}) = -10\log\,(T/(1-R)) = 10\log\,((1 - |S_{11}|^2)/\,|S_{21}|^2)$$

$$SE_T = SE_R + SE_A = -10\log(|S_{21}|^2)$$

where SE_A is the microwave absorption, SE_R is the microwave reflection, and SE_M is the microwave multiple internal reflection.

Fig. 9 represents the electromagnetic shielding behavior for the MXene-PANI composite showing various shielding effectiveness’ (due to reflection, absorption and total) with respect to X-band frequency range. It can be observed that highest value of total shielding effectiveness is 22.7 dB at the frequency 10.8 GHz and also the total effectiveness is almost constant with value of 21–22 dB in the entire frequency range. Also the shielding effectiveness’ due to absorption and

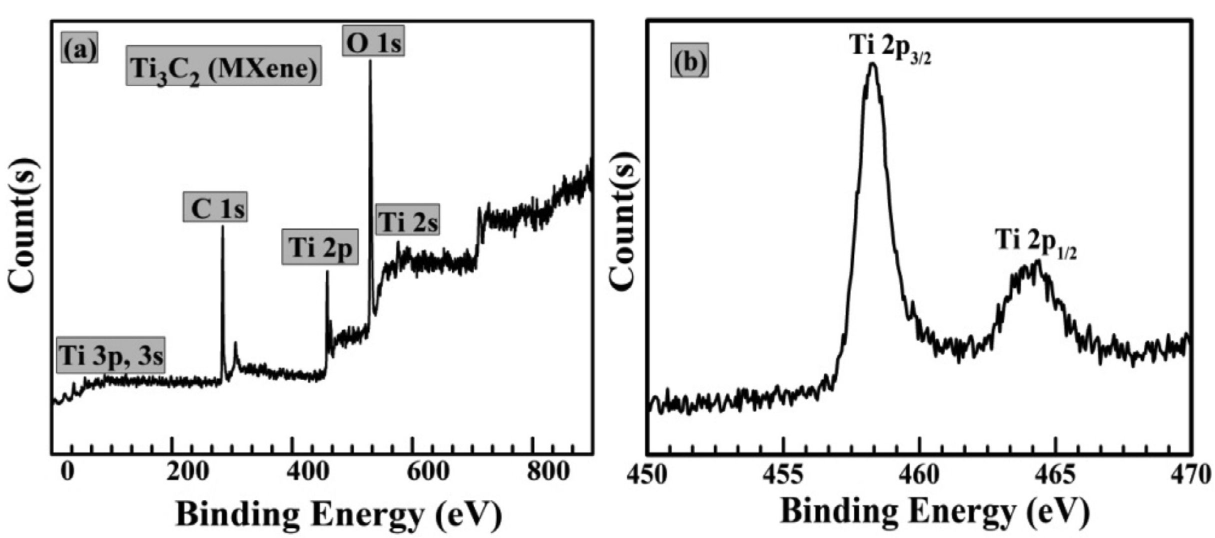

Fig. 5. (a) XPS survey spectrum of Ti_3C_2 and related high resolution (b) Ti 2p spectra of Ti_3C_2.

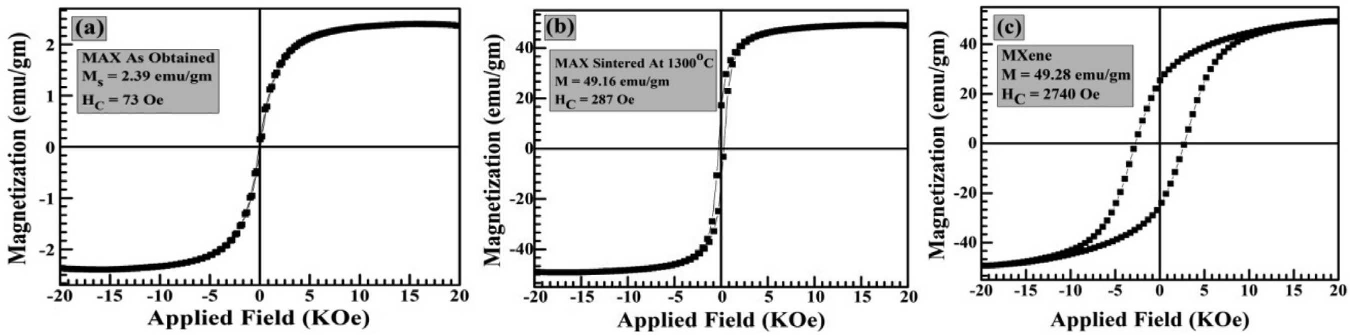

Fig. 6. M-H Loops of (a) As obtained Ti_3AlC_2 (b) Annealed Ti_3AlC_2 (c) Ti_3C_2 with applied magnetic field up to 2 T at room temperature.

Table 1
Magnetic Parameters, saturation magnetization and coercivity of samples at room temperature.

Compound	Ms (emu/gm)	Coercivity (Oe)
As obtained Ti_3AlC_2	2.39	73
Annealed Ti_3AlC_2	49.16	287
Ti_3C_2	49.28	2740

reflection are almost constant with values lying in the range of 16–18 dB and 4–5 dB respectively. This shows that the composite has sustainable microwave absorption properties in X-band. The EMI shielding originates from the excellent electrical conductivity and the layered architecture of the MXene. As electromagnetic radiations (EMRs) strike the surface of the sample, some EM waves are immediately reflected because of abundant free electrons at the surface of the highly conductive MXene [24,40,41]. The remaining waves pass through the MXene layered structure where interaction with the high electron density of MXene induces currents that contribute to ohmic losses, resulting in a drop in energy of the EMRs. The remaining EMRs, after passing through the first layer of Ti_3C_2 encounter the next barrier layer and the phenomenon of EMW attenuation continues. The EMRs

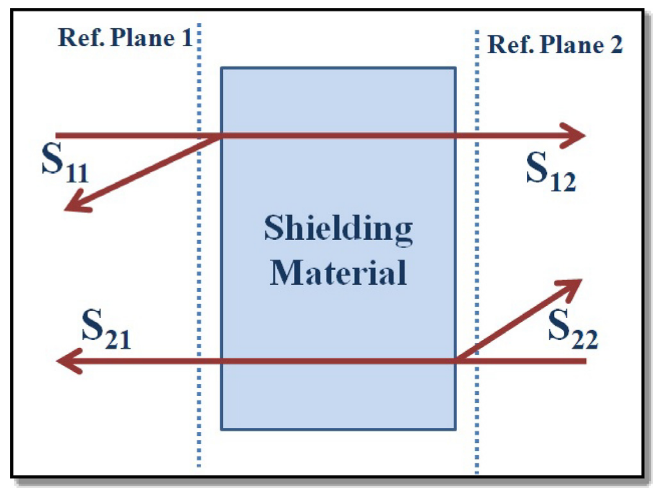

Fig. 8. Demonstration of S parameters along a shielding material in a vector network analyzer.

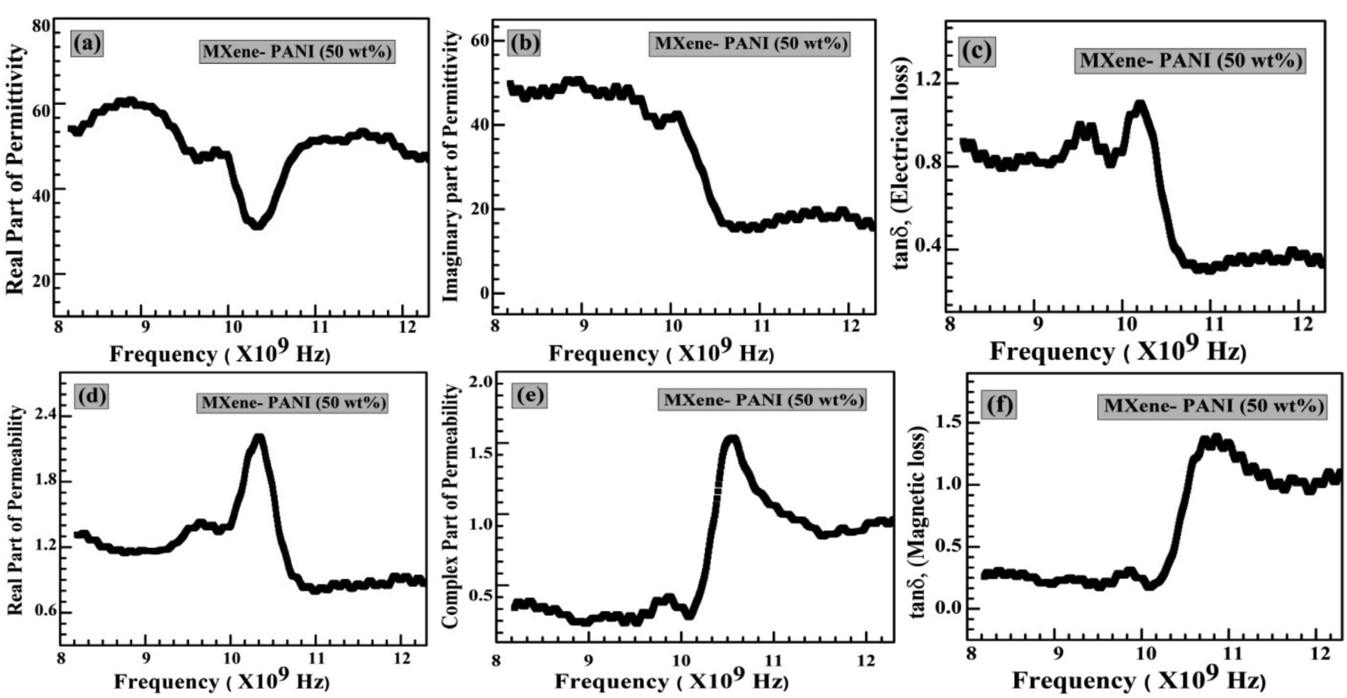

Fig. 7. Variation of (a, b) complex permitivity, (c) electrical tangent loss, (d, e) complex permeability and (f) magnetic tangent loss of Ti_3C_2 - PANI composite with respect to frequency in X-band.

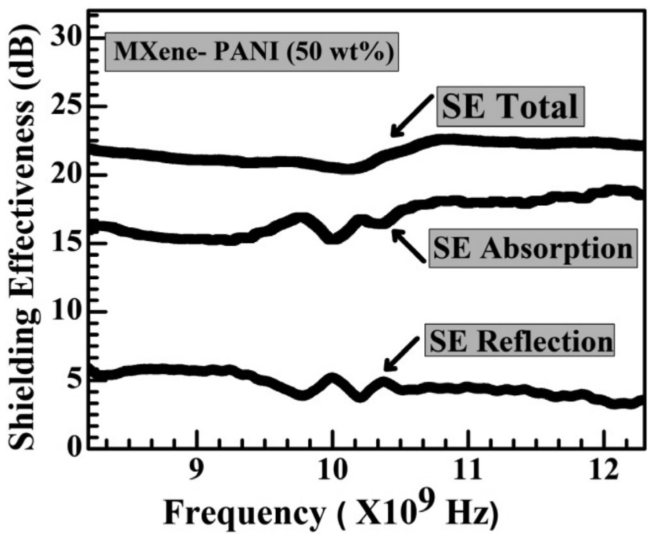

Fig. 9. Shielding Effectiveness (SE_R, SE_A and SE_T) in X band frequency range for Ti_3C_2-PANI composite.

can be reflected back and forth between the layers until completely absorbed in the structure whereas in pure metals that have a regular crystallographic structure, no interlayer reflecting surface is available to provide the internal multiple reflection phenomenons. So far, most research has focused on graphene [42,43], carbon nanotubes [44], iron oxides [45], ferrites [46], iron aluminum-silicon alloys [47], and metallic-based filler [48] polymer composites. To explore the EMI shielding properties of MXenes, we studied shielding effectiveness of the composite of Ti_3C_2 with polyaniline. Ti_3C_2 with the good electrical conductivity gives the better EMI shielding effectiveness among the studied MXenes [49–51]. The composite of MXene with PANI may lead us to cost effective, low weight and sustainable EMI shielding material.

4. Conclusions

We report the fabrication of lightweight, cost effective and sustainable composite of MXene and PANI with excellent EMI-shielding performance. We have synthesized MXene Ti_3C_2 by exfoliation of ternary carbides Ti_3AlC_2 in aqueous solution of HF and composites of Ti_3C_2 with polyaniline by mechanical blending. The magnetic properties of MAX Ti_3AlC_2 and MXene Ti_3C_2 have been reported first time which show a good ferromagnetic behavior for both the samples. High electrical conductivity and magnetization (49 emu/gm) of Ti_3C_2 sample make it suitable filler in polymer matrix. The EMI shielding behavior of Ti_3C_2-PANI composite has been intensively studied over the frequency range of X-band. The Ti_3C_2-PANI composite showed an excellent shielding effectiveness with almost steady value of 21–23 dB in the entire X-band frequency range which makes it a suitable candidate as EMI shielding material.

Acknowledgments

Authors are thankful to Physics Department, Hindu College, University of Delhi and Head, Department of Physics and Astrophysics, University of Delhi. We acknowledge the University Science Instrumental Centre (USIC), University of Delhi and National Physical Laboratory (NPL), New Delhi for the characterization facilities.

Appendix A. Supplementary data

Supplementary data to this article can be found online at https://doi.org/10.1016/j.jmmm.2019.165364.

References

[1] K.J. Vinoy, R.M. Jha, Radar Absorbing Materials, From Theory to Design and. Characterization, Boston, 1996.
[2] F. Brosseau Qin, A review and analysis of microwave absorption in polymer composites filled with carbonaceous particles, J. Appl. Phys. 111 (2012) 061301–61324, https://doi.org/10.1063/1.3688435.
[3] M.S. Cao, W.L. Song, Z.L. Hou, B. Wen, J. Yuan, The effects of temperature and frequency on the dielectric properties, electromagnetic interference shielding and microwave-absorption of short carbon fiber/silica composites, Carbon 48 (2010) 788–796, https://doi.org/10.1016/j.carbon.2009.10.028.
[4] M. Sundararaj Arjmand, Effects of nitrogen doping on x-band dielectric properties of carbon nanotube/polymer nanocomposites, ACS Appl. Mater. Interfaces 7 (2015) 17844–17850, https://doi.org/10.1021/acsami.5b04211.
[5] Q. Liu, Q. Cao, H. Bi, C. Liang, K. Yuan, W. She, Y. Yang, R. Che, CoNi@SiO_2@TiO_2 and CoNi@Air@TiO_2 microspheres with strong wideband microwave absorption, Adv. Mater. 28 (2016) 486–490, https://doi.org/10.1002/adma.201503149.
[6] Yi Zhang, Y. Yi Huang, T. Zhang, H. Chang, P. Xiao, H. Chen, Z Chen Huang, Broadband and tunable high-performance microwave absorption of an ultralight and highly compressible graphene foam, Adv Mater. 27 (2015) 2049–2053, https://doi.org/10.1002/adma.201405788.
[7] H. Al-Saleh Mohammed, H. Saadeh Walaa, Uttandaraman Sundararaj, EMI shielding effectiveness of carbon based nanostructured polymeric materials: a comparative study, Carbon 60 (2013) 146–156, https://doi.org/10.1016/j.carbon.2013.04.008.
[8] Hae-Rim Kim, Kazushige Fujimori, Byoung-Suhk Kim, Ick-Soo Kim, Lightweight nanofibrous EMI shielding nanowebs prepared by electrospinning and metallization, Compos. Sci. Technol. 72 (2012) 1233–1239, https://doi.org/10.1016/j.compscitech.2012.04.009.
[9] Bo Wen, Mao-Sheng Cao, Zhi-Ling Hou, Lu Wei-Li Song, Ming-Ming Lu Zhang, Hai-Bo Jin, Xiao-Yong Fang, Wen-Zhong Wang, Jie Yuan, Temperature dependent microwave attenuation behavior of carbon-nanotube/silica composites, Carbon 6 (2013) 124–139, https://doi.org/10.1016/j.carbon.2013.07.110.
[10] Xiaosi Qi, Xu. Jianle, Hu. Qi, Yu. Deng, Ren Xie, Yang Jiang, Wei Zhong, Du. Youwei, Metal-free carbon nanotubes: synthesis and enhanced intrinsic microwave absorption properties, Sci. Rep. 6 (2016) 28310, https://doi.org/10.1038/srep28310.
[11] Meikang Han, Xiaowei Yin, Sa. Ren, Wenyan Duan, Litong Zhang, Laifei Cheng, Core/shell structured C/ZnO nanoparticles composites for effective electromagnetic wave absorption, RSC Adv. 6 (2016) 6467–6474, https://doi.org/10.1039/C5RA25295D.
[12] Zhihui Zeng, Mingji Chen, Yongmao Pei, Seyed Ismail Seyed Shahabadi, Boyang Che, Peiyu Wang, Lu. Xuehong, Ultralight and flexible polyurethane/silver nanowire nanocomposites with unidirectional pores for highly effective electromagnetic shielding, ACS Appl. Mater. Interfaces 9 (2017) 32211–32219, https://doi.org/10.1021/acsami.7b07643.
[13] Yan Wang, Gu. Fu-qiang, Li-juan Ni, Kun Liang, Kyle Marcus, Shu-li Liu, Fan Yang, Jin-ju Chen, Zhe-sheng Feng, Easily fabricated and lightweight PPy/PDA/AgNW composites for excellent electromagnetic interference shielding, Nanoscale 9 (2017) 18318–18325, https://doi.org/10.1039/C7NR05951E.
[14] Wei-Li Song, Mao-Sheng Cao, Lu Ming-Ming, Song Bi, Chan-Yuan Wang, Jia Liu, Jie Yuan, Li-Zhen Fan, Flexible graphene/polymer composite films in sandwich structures for effective electromagnetic interference shielding, Carbon 66 (2014) 67–76, https://doi.org/10.1016/j.carbon.2013.08.043.
[15] Aboutaleb Ameli, Mohammadreza Nofar, Sai Wang, Chul B. Park, Lightweight polypropylene/stainlesssteel fiber composite foams with low percolation for efficient electromagnetic interference shielding, ACS Appl. Mater. Interfaces 6 (2014) 11091–11100, https://doi.org/10.1021/am500445g.
[16] He Ji, Rui Zhao, Nan Zhang, Changxian Jin, Lu. Xiaofeng, Ce Wang, Lightweight and flexible electro spun polymer nanofiber/metal nanoparticle hybrid membrane for high performance electromagnetic interference shielding, NPG Asia Materials 10 (2018) 749–760, https://doi.org/10.1038/s41427-018-0070-1.
[17] M. Naguib, V.N. Mochalin, M.W. Barsoum, Y. Gogotsi, MXenes: a new family of two-dimensional materials, Adv. Mater. 26 (2014) 992–1005, https://doi.org/10.1002/adma.201304138.
[18] F. Shahzad, M. Alhabeb, C.B. Hatter, B. Anasori, S.M. Hong, C.M. Koo, Y. Gogotsi, Electromagnetic interference shielding with 2D transition metal carbides (MXenes), Science 353 (2016) 1137–1140, https://doi.org/10.1126/science.aag2421.
[19] A. Lipatov, M. Alhabeb, M.R. Lukatskaya, A. Boson, Y. Gogotsi, A. Sinitskii, Effect of synthesis on quality, electronic properties and environmental stability of individual monolayer Ti_3C_2 MXene flakes, Adv. Electron. Mater. 2 (2016) 1600255, https://doi.org/10.1002/aelm.201600255.
[20] A.D. Dillon, M.J. Ghidiu, L. Krick, J. Griggs, S.J. May, Y. Gogotsi, M.W. Barsoum, A.T. Fafarman, Highly conductive optical quality solution-processed films of 2D titanium carbide, Adv. Funct. Mater. 26 (2016) 4162–4168, https://doi.org/10.1002/adfm.201600357.
[21] Zheng Ling, Chang E. Ren, Meng-Qiang Zhao, Jian Yang, James M. Giammarco, Jieshan Qiu, Michel W. Barsoum, Yury Gogotsi, Flexible and conductive MXene films and nanocomposites with high capacitance, PNAS 111 (2014) 16676–16681, https://doi.org/10.1073/pnas.1414215111.
[22] Muhammad Boota, Babak Anasori, Cooper Voigt, Meng-Qiang Zhao, Michel W. Barsoum, Yury Gogotsi, Pseudocapacitive electrodes produced by oxidant-free polymerization of pyrrole between the layers of 2D titanium carbide (MXene), Adv. Mat. 28 (2016) 1517–1522, https://doi.org/10.1002/adma.201504705.
[23] B. Anasori, M.R. Lukatskaya, Y. Gogotsi, 2D metal carbides and nitrides (MXenes)

for energy storage, Nat. Rev. Mater. 2 (2017) 16098, https://doi.org/10.1038/natrevmats.2016.98.
[24] M. Naguib, M. Kurtoglu, V. Presser, J. Lu, J. Niu, M. Heon, L. Hultman, Y. Gogotsi, M.W. Barsoum, Two-dimensional nanocrystals produced by exfoliation of Ti_3AlC_2, Adv. Mater. 23 (2011) 4248–4253, https://doi.org/10.1002/adma.201102306.
[25] Olha Mashtalir, Michael Naguib, Boris Dyatkin, Yury Gogotsi, Michel W. Barsoum, Kinetics of aluminum extraction from Ti_3AlC_2 in hydrofluoric acid, Mater. Chem. Phys. 139 (2013) 147–152, https://doi.org/10.1016/j.matchemphys.2013.01.008.
[26] Zh.A. Boeva, V.G. Sergeyev, polyaniline: synthesis: properties, and application, Polymer Science 56 (2014) 144–153, https://doi.org/10.1134/S1811238214010032.
[27] Akheel A. Syed, Maravattickal K. Dinesan, Review: Polyaniline—A novel polymeric material, Talanta 38 (1991) 815–837, https://doi.org/10.1016/0039-9140(91)80261-W.
[28] J. Liu, H.B. Zhang, R. Sun, Y. Liu, Z. Liu, A. Zhou, Z.Z. Yu, Hydrophobic, flexible, and lightweight MXene foams for high-performance electromagnetic-interference shielding, Adv. Mater. 29 (2017) 1702367doi:10.1002/adma.201702367.
[29] Jin Yang, Beibei Chen, Haojie Song, Hua Tang, Changsheng Li, Synthesis, characterization, and tribological properties of two-dimensional Ti_3C_2, Cryst. Res. Technol. 49 (2014) 926–932, https://doi.org/10.1002/crat.201400268.
[30] Ravuri Syamsai, Pratap Kollu, Soon Kwan Jeong, Andrews Nirmala Grace, Synthesis and properties of 2D-titanium carbide MXene sheets towards electrochemical energy storage applications, Ceramics Int. 43 (2017) 13119–13126, https://doi.org/10.1016/j.ceramint.2017.07.003.
[31] S.-B. Li, H.-X. Zhai, G.P. Bei, Y. Zhou, Z.L. Zhang, Formation of Ti_3AlC_2 by mechanically induced self-propagating reaction in Ti–Al–C system at room temperature, Mater. Sci. Technol. 22 (2006) 667–672, https://doi.org/10.1179/174328406X91050.
[32] M.R. Lukatskaya, O. Mashtalir, C.E. Ren, Y. Dall'Agnese, P. Rozier, P.L. Taberna, M. Naguib, P. Simon, M.W. Barsoum, Y. Gogotsi, Cation intercalation and high volumetric capacitance of two-dimensional titanium carbide, Science 341 (2013) 1502–1505, https://doi.org/10.1126/science.1241488.
[33] M. Naguib, O. Mashtalir, J. Carle, V. Presser, J. Lu, L. Hultman, Y. Gogotsi, M.W. Barsoum, Two-dimensional transition metal carbides, ACS Nano 6 (2012) 1322–1331, https://doi.org/10.1021/nn204153h.
[34] X. Jian, B. Wu, Y. Wei, S.X. Dou, X. Wang, W. He, N. Mahmood, Facile synthesis of Fe_3O_4/GCs composites and their enhanced microwave absorption properties, ACS Appl. Mater. Interfaces 8 (2016) 6101–6109, https://doi.org/10.1021/acsami.6b00388.
[35] M. Mo, L. Zhang, G. Wang, Characteristics of dielectric behavior in nanostructured materials, Nanostruct. Mater. 6 (1995) 823–826, https://doi.org/10.1016/0965-9773(95)00186-7.
[36] B. Lu, X.L. Dong, H. Huang, X.F. Zhang, X.G. Zhu, J.P. Lei, Microwave absorption properties of the core/shell-type iron and nickel nanoparticles, J. Magn. Magn. Mater. 320 (2008) 1106–1111, https://doi.org/10.1016/j.jmmm.2007.10.030.
[37] Peijiang Liu, Zhengjun Yao, Vincent Ming Hong Ng, Jintang Zhou, Ling Bing Kong, Kan Yuea, Facile synthesis of ultrasmall Fe_3O_4 nanoparticles on MXenes for high microwave absorption performance, Composites Part A 115 (2018) 371–382, https://doi.org/10.1016/j.compositesa.2018.10.014.
[38] Wen-Tao Cao, Fei-Fei Chen, Ying-Jie Zhu, Yong-Gang Zhang, Ying-Ying Jiang, Ming-Guo Ma, Feng Chen, Binary strengthening and toughening of MXene/cellulose nanofiber composite paper with nacre-inspired structure and superior electromagnetic interference shielding properties, ACS Nano 12 (2018) 4583–4593, https://doi.org/10.1021/acsnano.8b00997.
[39] S.K. Dhawan, Kuldeep Singh, A.K. Bakhshi, Anil Ohlan, Conducting polymer embedded with nanoferrite and titanium dioxide nanoparticles for microwave absorption, Synthetic Metals 159 (2009) 2259–2262, https://doi.org/10.1016/j.synthmet.2009.08.031.
[40] H.B. Zhang, Q. Yan, W.G. Zheng, Z. He, Z.Z. Yu, Tough graphene – polymer microcellular foams for electromagnetic interference shielding, ACS Appl. Mater. Interfaces 3 (2011) 918–924, https://doi.org/10.1021/am200021v.
[41] Jean-Michel Thomassin, Christine Jérôme, Thomas Pardoen, Christian Bailly, Isabelle Huynen, Christophe Detrembleur, Polymer/carbon based composites as electromagnetic interference (EMI) shielding materials, Mater. Sci. Eng. Rep. 74 (2013) 211–232, https://doi.org/10.1016/j.mser.2013.06.001.
[42] Jiajie Liang, Yan Wang, Yi Huang, Yanfeng Ma, Zunfeng Liu, Jinming Cai, Chendong Zhang, Hongjun Gao, Yongsheng Chen, Electromagnetic interference shielding of graphene/epoxy composites, Carbon 47 (2009) 922–925, https://doi.org/10.1016/j.carbon.2008.12.038.
[43] F. Shahzad, P. Kumar, Y.-H. Kim, S.M. Hong, C.M. Koo, Biomass-derived thermally annealed interconnected sulfur-doped graphene as a shield against electromagnetic interference, ACS Appl. Mater. Interfaces 8 (2016) 9361–9369, https://doi.org/10.1021/acsami.6b00418.
[44] Zhihui Zeng, Mingji Chen, Hao Jin, Weiwei Li, Xiao Xue, Licheng Zhou, Yongmao Pei, Hui Zhang, Zhong Zhang, Thin and flexible multi-walled carbon nanotube/waterborne polyurethane composites with high-performance electromagnetic interference shielding, Carbon 96 (2016) 768–777, https://doi.org/10.1016/j.carbon.2015.10.004.
[45] S. Varshney, A. Ohlan, V.K. Jain, V.P. Dutta, S.K. Dhawan, In situ synthesis of polypyrrole-γ-Fe_2O_3-Fly ash nanocomposites for protection against EMI pollution, Ind. Eng. Chem. Res. 53 (2014) 14282–14290, https://doi.org/10.1021/ie500512d.
[46] Xu. Ping, Xijiang Han, Chao Wang, Hongtao Zhao, Jingyu Wang, Xiaohong Wang, Bin Zhang, Synthesis of electromagnetic functionalized barium ferrite nanoparticles embedded in polypyrrole, J. Phys. Chem. B 112 (2008) 2775–2781, https://doi.org/10.1021/jp710259v.
[47] L. Liu, Z.H. Yang, C.R. Deng, Z.W. Li, M.A. Abshinova, L.B. Kong, High frequency properties of composite membrane with in-plane aligned Sendust flake prepared by infiltration method, J. Magn. Magn. Mater. 324 (2012) 1786–1790, https://doi.org/10.1016/j.jmmm.2011.12.038.
[48] A. Ameli, M. Nofar, S. Wang, C.B. Park, Lightweight polypropylene/stainless-steel fiber composite foams with low percolation for efficient electromagnetic interference shielding, ACS Appl. Mater. Interfaces 6 (2014) 11091–11100, https://doi.org/10.1021/am500445g.
[49] Qing Yuchang, Zhou Wancheng, Luo Fa, Zh.u. Dongmei, Titanium carbide (MXene) nanosheets as promising microwave absorbers, Ceramics Int. 42 (2016) 16412–16416, https://doi.org/10.1016/j.ceramint.2016.07.150.
[50] H. Yang, J. Dai, X. Liu, Y. Lin, J. Wang, L. Wang, F. Wang, Layered PVB/$Ba_3Co_2Fe_{24}O_{41}$/Ti_3C_2 Mxene composite: Enhanced electromagnetic wave absorption properties with high impedance match in a wide frequency range, Mater. Chem. Phys. 200 (2017) 179–186, https://doi.org/10.1016/j.matchemphys.2017.05.057.
[51] Xinli Liu, Wu. Jisi, Jun He, Lei Zhang, Electromagnetic interference shielding effectiveness of titanium carbide sheets, Mater. Lett. 205 (2017) 261–263, https://doi.org/10.1016/j.matlet.2017.06.101.